

This paper reports the results of experimental studies into determining mechanical properties (elastic and dissipative) at the shear of the material of a pressure fire hose of the "T" type with the internal diameter of 77 mm using torsion tests. During the studies, a series of field experiments have been conducted on the torsion of the pressure fire hose samples with internal hydraulic pressure (P) in a hose of 0.2 MPa (P1), 0.4 MPa (P2), and 0.6 MPa (P3) under conditions of static loading-unloading cycles. The tests consisted of 6 cycles – for each of the (P) loading-unloading cycles, which were carried out at a two-minute interval, the rigidity and elasticity modules at the shear of the material of a hose were determined by means of torsion tests. It was established that the numerical results of mechanical properties depend on the hose load "history", that is, the elasticity modules increased in the first two, three load cycles, and they stabilized only afterward at the level of 3.04 MPa for P1, 4.35 MPa for P2, 4.39 MPa for P3. The above, together with a significant decrease in residual deformations, strengthens the elastic properties of the fire hose material.

The results of the research have been approximated by the corresponding trend lines. The equation of dependence of the current torque on deformation was determined. The curves of the deformation of samples, which, under the conditions of cyclic loading-unloading, formed hysteresis loops, were established. The resulting hysteresis loops during the study in the first two modes undergo quantitative and qualitative changes, namely, the slope and its area decrease. The similarity of experimental studies at different internal pressures (P) was established.

A change in the properties of the material of a fire hose at the consecutive loading-unloading deformation cycles is reverse, the gaps between the deformation cycles lead to a partial restoration of the mechanical characteristics, approximating them to the original values

Keywords: pressure fire hose, working pressure, elasticity module, hysteresis, dissipative properties, torsion

DETERMINING MECHANICAL PROPERTIES AT THE SHEAR OF THE MATERIAL OF "T" TYPE PRESSURE FIRE HOSE BASED ON TORSION TESTS

S. Nazarenko

PhD

Department of Engineering and Rescue Machinery*

E-mail: itaart.nazarenko@gmail.com

R. Kovalenko

PhD

Department of Engineering and Rescue Machinery*

V. Asotskyi

Researcher

Department of Organization and Coordination of Research Activities

Scientific-Methodical Center of Educational Institutions in

the Sphere of Civil Defence

O. Gonchara str., 55a, Kyiv, Ukraine, 01601

G. Chernobay

PhD, Associate Professor

Department of Applied Mechanics and Environmental Technologies*

A. Kalynovskyi

PhD, Associate Professor

Department of Engineering and Rescue Machinery*

I. Tseabriuk

PhD, Associate Professor**

O. Shapovalov

PhD**

I. Shasha

Doctor of Technical Sciences**

V. Demianyshyn

PhD**

A. Demchenko

PhD

Department of organization of scientific activity

Cherkasy Institute of Fire Safety named after the Heroes of Chernobyl

Onoprienka str., 8, Cherkasy, Ukraine, 18034

*National University of Civil Defence of Ukraine

Chernyshevskaya str., 94, Kharkiv, Ukraine, 61023

**Department of Armored Vehicles

National Academy of National Guard of Ukraine
Zakhysnykiv Ukrainy sq., 3, Kharkiv, Ukraine, 61001

Received date 27.04.2020

Accepted date 10.09.2020

Published date 23.10.2020

Copyright © 2020, S. Nazarenko, R. Kovalenko, V. Asotskyi, G. Chernobay,

A. Kalynovskyi, I. Tseabriuk, O. Shapovalov, I. Shasha, V. Demianyshyn, A. Demchenko

This is an open access article under the CC BY license (<http://creativecommons.org/licenses/by/4.0>)

1. Introduction

For a long time, fires have been one of the main problems that posed a danger to the life and health of the planet population. According to [1], in the structure of calls of emergency rescue units (ERU), today fires occur more frequently

compared to other types of hazardous events and emergencies. The facts, when fires devastated entire cities, and their inhabitants could not effectively counteract this disaster, are known from history.

First motor vehicles and specialized fire and technical equipment (FTE) for firefighting began to appear with

the development of the science of engineering. In case of extremely complex fires, such as landscape fires [2], or hazardous sites, the ERU uses a large number of FTE. However, successful works on fire extinguishing by the ERU depends not only on the time of concentration of forces and facilities on the place of a call [1] but also on indicators of faultless work of the FTE [3]. The list of FTE includes an absorbing net, a fire column, fire hoses, branching, fire barrels, and other auxiliary equipment. According to statistics [4], fire hoses are the least reliable among the previously indicated equipment. Fire hoses are flexible pipelines, which are equipped with connecting heads at the ends and are designed for the transportation of fire-extinguishing substances. They are divided into suction, pressure-suction, and pressure hoses. The first two types of hoses are used to transport fire extinguishing agents under rarefaction when they are taken by fire pumps from an open water source or an external water supply network. Fire hoses of the third type are designed to transport fire extinguishing agents under excessive pressure to fire barrels. Returning to the issue of FTE reliability, pressure fire hoses (PFH) are the least reliable among the three types of fire hoses [4]. PFH failures may be caused by production defects in their design, violation of storage, and testing conditions. In the process of fire extinguishing, punctures, cuts, ruptures, burn-outs, and loosening of fixing connecting heads are added to the specified list of failure causes.

In order to prevent a failure during the operation, the PFHs are periodically subject to hydraulic tests for tightness by creating excess pressure in their inner cavity. This method of testing makes it possible to detect only existing external damage, while its main drawback is that it does not make it possible to detect internal defects of the material the PFH is made of.

Thus, ensuring the PFH reliability in the process of fire extinguishing requires compliance with the proper conditions of their operation, in particular, periodic tests. The method for PFH testing, which is used by the ERU, does not make it possible to identify their hidden defects. Accordingly, the development of a new method for PFH testing, which will make it possible to detect their hidden defects is an important scientific and practical task.

2. Literature review and problem statement

Paper [3] proposed a systematic approach and the principle of assessing the ERU readiness for operational actions. It is believed that a unit is ready to perform operational actions, provided it has the necessary amount of technically efficient equipment in good working conditions, and trained personnel staffed according to the staff list. At the same time, the probabilities that the ERUs have an appropriate type of equipment in proper quantity, the equipment is in good condition, as well as the probability of its faultless operation in the process of operational actions, are also taken into account. Accordingly, the total indicator of ERU readiness to perform operative actions will depend on the technical conditions of PFH as one of the kinds of FTE, which was not considered in paper [3].

In order to prevent the failure of PFHs during operation, their technical condition is periodically diagnosed. In the ERU subdivisions, hydraulic PFH tightness testing is the basic method of diagnosis, as it was indicated earlier.

A well-known method for diagnosing the technical condition of flexible pipelines, in particular, high-pressure hydraulic hoses, is the method that implies the application of industrial computer tomography. According to [5], the above method has the limitation, which involves the necessity to pre-checking the possibility of its use for a specific type of a high-pressure hydraulic hose. This is due to the fact that high-pressure hydraulic hoses can be, like PFH, multi-layered, and the material of which corresponding layers are made can also be composite. Taking into consideration the specified limitation of this method of diagnosis, we can conclude that it is not universal and cannot be applied to diagnose the technical condition of all existing types of PFH.

During the operation, the PFHs are often in a prolonged strain-deformed state, accompanied by intense fatigue of the material from which they are made. Intense fatigue contributes to changes in the properties of the PFH material, the emergence and development of cracks and their destruction after a certain time. In article [6], it is proposed to use the homogenization and interpolation methods to simulate and analyze the deformations of flexible pipelines of the hydraulic brake system of a car. Established mathematical dependences, obtained with the use of these methods, make it possible to predict the areas with deformations in a flexible pipeline and, consequently, to identify the probable places of damage. At the same time, article [6] points out the low accuracy of the proposed approach, which is related to the use of a rather simple model that cannot successfully reproduce the deformation of a flexible pipeline, taking into consideration its structure. A similar problem, which is associated with the identification of hidden defects in flexible pipelines caused by fatigue of material, is solved in research [7]. In this paper, the cycles of deformation and stress in different variations are calculated by counting the rain stream cycles, and the life cycle of fatigue is evaluated by three models of fatigue resource evaluation. Certain admissions were made in the paper, given that flexible pipelines, studied in the research, consist of the layers of rubber and fabric weaving. In particular, fatigue processes that occur only in the rubber layer were studied in the paper, while fatigue processes occurring in a woven fabric layer were not taken into consideration. These assumptions in the process of research in paper [7] do not make it possible to assert the high accuracy of obtained results and their reliability, which casts doubt on the feasibility of using these methods in practice.

Article [8] examines the nature of deformation caused by loading and assesses the internal pressure, at which there occurs destruction of a flexible pipeline, depending on the weaving structure of its reinforcing layer. Among the types of deformation, we considered stretching and torsion of a flexible pipeline under the influence of growing pressure inside it. Simple kinds of weaving were considered as textile reinforcement. Established dependences were described by mathematical models. However, the paper did not examine the nature of the deformations of flexible pipelines in the presence of mechanical damages, which could be used in the diagnosis of the technical condition of PFH.

Mathematical models for calculation of ruptured hydraulic pressure in the internal cavity of PFH were proposed in papers [9, 10]. The models took into consideration such indicators as tension in the weft thread at rupture, the PFH radius, geometric densities on the warp and the weft of fabric shell of the PFH, diameters of threads, and coefficients of their vertical creasing. In addition to these indicators, math-

emathical models also took into consideration the coefficients that characterize the length of the contact zones between threads in shares of diameters of warp and weft threads. Accordingly, these mathematical models can be used only in designing new types of PFH.

A mathematical model of the process of accumulation of unlocalized fatigue damage in rubber-like materials is proposed in [11]. This mathematical model makes it possible to predict the probable size of fatigue damage but does not allow determining a specific place of their occurrence. This restriction does not enable the application of the mathematical model [11] in the process of diagnosing the technical condition of the PFH in order to identify hidden defects in them.

In the process of PFH stretching, there is self-heating of the material they are made of, which is the reason for changing their properties and leads to the appearance of residual deformations and hidden damages. Stretching of PFH occurs during putting the hose lines on vertical surfaces. Paper [12] contains the study of dissipative characteristics of rubber-based composite materials under the influence of cyclic loads taking into consideration the peculiarities of their self-heating. The samples were stretched under the influence of lengthy cyclic loading. The flat samples of rubber-based material with reinforcing fibers inside were used in the study. As a result, dependences of the temperature of the stabilization of the thermal condition of the studied samples on load conditions were obtained. In addition, the dependences of the loss module, dissipation factor, and relaxation time on load frequency, amplitude of deformations, and self-heating temperature of material were established. If we consider the actual process of PFH self-heating, it is necessary to take into consideration the fact that inside it there is a circulation of water, which cools down the material it is made of. Accordingly, the previously described conditions of the experiment [12] with the sample of rubber-based composite material do not correspond to actual conditions, in which stretching and self-heating of PFH occur. For these reasons, the research results shown in paper [12] cannot be used in the process of diagnosing the technical condition of the PFH. Similar studies were conducted in paper [13]. The segments of the PFH of the "T" type with the internal diameter of 66 mm were used as samples. The tests consisted of 5 loading-unloading cycles, which were conducted at a two-minute interval. Taking into consideration the experimental data, the elasticity module at stretching the NPR material in the longitudinal direction was determined. In article [13] it was found that under the influence of static load, there was a change in the physical properties of the material and the occurrence of residual deformation. The peculiarity of this process is its reverse character, that is, a partial restoration of the physical properties of the material from which the PFH is made after a certain time of the unloading cycle. Accordingly, the results of research [13] make it possible to understand the behavior of PFH material at its longitudinal stretching, but cannot be used to find their hidden defects.

In the practice of using PFHs by ERUs, there are cases of their being influenced by automotive fuel, which is possible in the case of extinguishing fires and carrying out rescue work at the sites of transport, oil production, and storage of petroleum products.

According to [14], during the influence on the elastomers, which are part of PFH of automotive fuel, there is a change in their physical properties. This work examined the impact on diesel and biodiesel fuel on the physical

properties of elastomers. The study was conducted by static immersion of elastomer samples into diesel and biodiesel fuel for the time of 1,000 units. The weight and volume, hardness, and resistance to rupture of the studied samples were measured every 250 hours. During the experiment cycle, there was a process in changing the chemical composition of the fuel, in which the experimental sample of elastomer was immersed, which was established by methods of gas chromatography with mass spectroscopy. The results of the research established the types of elastomers, which have high resistance to the influence of diesel and biodiesel fuel compared to other samples. These results can be used in the process of determining the technical condition of the PFHs, which have been in contact with spilled fuel, provided that the composition of the material from which they are made is known.

Paper [15] studied the causes of the damage to flexible pipelines of the hydraulic amplifier of vehicle steering control. According to the results of these studies, it was found that most losses of brake fluid from flexible pipelines occur in the places of mounting connecting fittings on them. The causes of these losses are sharp corners of the bush, which damages the outer rubber layer of a pipeline. In research [16], it was found that the causes of leaks in the places of mounting connecting fittings, in addition to the previously indicated ones, are its destruction due to deviations in the production process. Similar damage is observed in the places of mounting connecting heads at the ends of the PFH, which is also associated with their production quality and the errors made during mounting. In papers [15, 16], the damage in the areas of connecting fitting [15, 16] was detected by obvious signs, that is, by the existing fluid leakage. Articles [15, 16] proposed recommendations to improve the quality of manufacturing connecting fittings. The specified articles do not contain the information on the necessity and order of diagnosing the technical condition of flexible pipelines and connecting fittings in order to prevent their failure during operation.

Thus, the analysis of literary sources [3–16] revealed that most studies are related to determining the causes of damage to flexible pipelines [8–10, 15, 16]. In addition, a series of works [7, 12–14] are related to the studies of the behavior of the material from which flexible pipelines are made at different influences on them. Only separate papers contain the methods that make it possible to establish [5, 6] or predict [11] possible damage to flexible pipelines, in particular PFH. Due to the found drawbacks and limitations of these methods, they cannot be applied effectively to diagnose the technical condition of the PFH. Accordingly, it becomes clear that the damage that arises in the materials from which flexible pipelines are made of generally affect a change of their physical properties. The indicated feature of the behavior of materials in the analyzed papers was little researched, which makes it possible to formulate the problems of these studies. To establish the fact of a change in physical properties of the material from which PFH is made in case of its damage, requires, first of all, conducting research into mechanical properties of the samples which were not damaged. To do this, it is necessary to study the mechanical properties of PFH of the "T" type with an internal diameter of 77 mm. The choice of this type and the diameter of hoses are explained by the highest frequency of use when laying the main hose lines during fire extinguishing.

3. The aim and objectives of the study

The aim of this study is to determine elastic and dissipative properties at the shear of the material of a pressure fire hose of the “T” type by means of torsion tests under conditions of static loading-unloading cycles at different pressure in a hose for subsequent calculations of their reliability.

To achieve the aim, the following tasks were set:

- to conduct experimental studies on determining the elastic properties at the shear of the material of a pressure fire hose by torsion tests;
- to conduct the experimental studies on determining the dissipative properties at the shear of the material of a pressure fire hose by means of torsion tests.

4. Procedure of experimental studies on determining the elastic and dissipative properties at the shear of the material of a pressure fire hose of the “T” type by torsion tests

During the study, we conducted a series of field experiments to determine elastic and dissipative properties when torsion the samples of new pressure fire hoses of the “T” type with the internal diameter of 77 mm under conditions of static loading-unloading cycles and statistical treatment of results.

In detail, the design of the PFH was considered in paper [13]. The experimental sample was separated from a fire hose of the “T” type with the inner diameter of 77 mm, the wall thickness $\delta=2.7$ mm that had the test length $L=0.980$ m.

The sample was fixed in an experimental setup in the upright position using cylindrical mechanical clamps. Rigid load, that is, fixed values of deformation of samples were assigned, while efforts were measured by a regular mechanical dynamometer. Before use, the dynamometer was tested by sequential loading using a reference dynamometer and subsequent construction of the corresponding characteristics and determining the required coefficients.

To conduct the corresponding works, we used the experimental setup, the scheme of which is shown in Fig. 1.

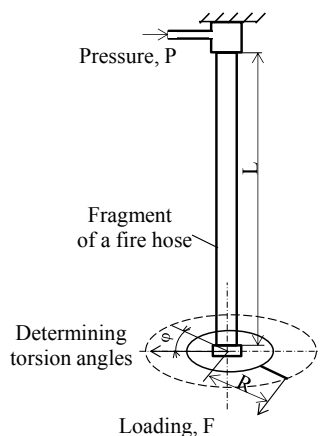


Fig. 1. Experimental setup with the mounted fragment on a fire hose

We performed the test cycles with its torsion relative to the longitudinal axis at an angle with a 60° pitch at the action of torque M_t , which is equal to the product of force load F (determined by a dynamometer) by the lever length $R=0.281$ m. The experiments were conducted in

two separate variants. First, the experiments on determining the elastic properties of PFH material at torsion were carried out. The second variant of the experiments were the tests to determine the viscous-elastic properties of the material.

Each experiment was conducted with the samples that were separated from different sections of different hoses, that is, at least 9 samples, with the following statistical treatment of the results, as well as to check their repeatability.

4.1. Experimental studies of elastic properties at the shear of the material of a pressure fire hose by torsion tests

The research was conducted at internal pressure (P) in the hose $P_1=0.2$ MPa, $P_2=0.4$ MPa and $P_3=0.6$ MPa repeated six times.

The research results at $P_1=0.2$ MPa are shown in Table 1.

The initial (1) loading cycle was carried out with a non-deformed fragment of a fire hose.

The maximal magnitude of deformation was $\Delta\phi_1^{\max} = 540^\circ$ at the load $M_1^{\max} = 17.2$ Nm. After unloading, residual deformation of the fragment was $\Delta\phi_1^{\text{res}} = 180^\circ$.

During repeated cycle 2 that was carried out 2 minutes after the first one, the maximum value of deformation was $\Delta\phi_2^{\max} = 420^\circ$ at load $M_2^{\max} = 20.4$ Nm. Residual deformation of the fragment after unloading was $\Delta\phi_2^{\text{res}} = 240^\circ$.

During the next loading (cycle 3), which was conducted 2 minutes after cycle 2, the maximum magnitude of deformation was $\Delta\phi_3^{\max} = 480^\circ$ at loading $M_3^{\max} = 25.52$ Nm. Residual deformation of the fragment after unloading was $\Delta\phi_3^{\text{res}} = 300^\circ$.

In the following loading cycles (4–6), which were conducted at similar two-minute intervals, the maximum magnitude of deformation was $\Delta\phi_{4-6}^{\max} = 780^\circ$ at loading $M_{4-6}^{\max} = 27.9$ Nm. Residual deformation of the fragment after unloading was $\Delta\phi_{4-6}^{\text{res}} = 300^\circ$.

Table 1

Results of testing the PFH at $P_1=0.2$ MPa of torsion deformation

Torsion angle ϕ , degrees	Pressure in a hose, $P_1=0.2$ MPa			
	Torque M , Nm			
	Cycle 1	Cycle 2	Cycle 3	Cycles 4–6
	N	N	N	N
0	0.00	–	–	–
60	2.59	–	–	–
120	3.77	–	–	–
180	5.25	0.00	–	–
240	7.25	4.31	0.00	–
300	9.34	6.59	4.58	0.00
360	11.3	8.87	6.53	5.33
420	13.65	11.05	9.32	7.65
480	15.65	13.34	11.77	9.63
540	17.20	16.15	14.41	12.08
600	–	20.40	18.61	15.25
660	–	–	22.75	21.20
720	–	–	25.52	25.34
780	–	–	–	27.90

Research results at $P_2=0.4$ MPa are given in Table 2.

The initial (1) loading cycle was performed with a non-deformed fragment of a fire hose.

The maximum magnitude of deformation was $\Delta\phi_1^{\max} = 480^\circ$ at loading $M_1^{\max} = 26.92$ Nm. Residual deformation of the fragment after unloading was $\Delta\phi_1^{\text{res}} = 120^\circ$.

During repeated cycle 2, which was conducted 2 minutes after cycle 1, the maximum magnitude of deformation was $\Delta\phi_2^{\max} = 540^\circ$ at loading $M_2^{\max} = 29.80$ Nm. Residual deformation of the fragment after unloading was $\Delta\phi_2^{\text{res}} = 180^\circ$.

Table 2

Results of NPR testing at $P_2=0.4$ MPa of torsion deformation

Torsion angle ϕ , degrees	Pressure in a hose, $P_2=0.4$ MPa			
	Torque M , Nm			
	Cycle 1	Cycle 2	Cycle 3	Cycles 4–6
	N	N	N	N
0	0.00	–	–	–
60	5.17	–	–	–
120	7.12	0.00	–	–
180	9.59	6.30	0.00	0.00
240	12.23	9.80	6.75	7.30
300	14.85	12.10	10.70	9.81
360	19.52	15.75	13.80	12.24
420	22.65	19.60	18.05	17.93
480	26.92	26.10	23.47	24.55
540	–	29.80	29.53	29.90

At the following loading (cycle 3), which was carried out 2 minutes after the second, the maximum magnitude of deformation was $\Delta\phi_3^{\max} = 540^\circ$ at loading $M_3^{\max} = 29.53$ Nm. Residual deformation of the fragment after unloading was $\Delta\phi_3^{\text{res}} = 180^\circ$.

In the following loading cycles (4–6), which were carried out at similar 2-minute intervals, the maximum magnitude of deformation was $\Delta\phi_{4-6}^{\max} = 540^\circ$ at loading $M_{4-6}^{\max} = 29.90$ Nm. Residual deformation of the fragment after unloading was $\Delta\phi_{4-6}^{\text{res}} = 180^\circ$.

Research results at $P_3=0.6$ MPa are shown in Table 3.

The initial (1) loading cycle was conducted with a non-deformed fragment of a fire hose.

The maximum magnitude of deformation was $\Delta\phi_1^{\max} = 480^\circ$ at loading $M_1^{\max} = 29.95$ Nm. Residual deformation of the fragment after unloading was $\Delta\phi_1^{\text{res}} = 120^\circ$.

In the repeated cycle 2, which was conducted 2 minutes after cycle 1, the maximum magnitude of deformation was $\Delta\phi_2^{\max} = 540^\circ$ at loading $M_2^{\max} = 32.4$ Nm. Residual deformation of the fragment after unloading was $\Delta\phi_2^{\text{res}} = 120^\circ$.

At the following loading (cycle 3), which was carried out 2 minutes after the second, the maximum magnitude of deformation was $\Delta\phi_3^{\max} = 540^\circ$ at loading $M_3^{\max} = 34.47$ Nm. Residual deformation of the fragment after unloading was $\Delta\phi_3^{\text{res}} = 120^\circ$.

In the following loading cycles (4–6), which were carried out at similar 2-minute intervals, the maximum magnitude of deformation was $\Delta\phi_{4-6}^{\max} = 540^\circ$ at loading $M_{4-6}^{\max} = 35.24$ Nm.

Residual deformation of the fragment was $\Delta\phi_{4-6}^{\text{res}} = 180^\circ$.

Table 3

Results of testing PFH at $P_3=0.6$ MPa of torsion deformation

Torsion angle ϕ , degrees	Pressure in a hose, $P_3=0.6$ MPa			
	Torque M , Nm			
	Cycle 1	Cycle 2	Cycle 3	Cycles 4–6
	N	N	N	N
0	0.00	–	–	–
60	6.4	–	–	–
120	8.64	0.00	0.00	0.00
180	11.2	9.29	9.01	9.24
240	14.0	11.1	11.7	12.1
300	16.72	15.27	14.52	14.56
360	20.37	19.41	18.37	18.9
420	23.71	23.4	22.2	22.53
480	29.95	28.91	28.46	28.67
540	–	32.4	34.47	35.24

4. 2. Results of experimental studies of elastic properties at the shear of the material of a pressure fire hose in torsion tests

The diagrams that correspond to statistically treated results of torsion tests of a pressure fire hose at internal pressure $P_1=0.2$ MPa are shown in Fig. 2, $P_2=0.4$ MPa are presented in Fig. 3, and $P_3=0.6$ MPa are shown in Fig. 4.

Analyzing the graphic part (Fig. 2–4) at different magnitudes of pressure in a hose, it is possible to accept in first approximation the dependence between loading and deformation of the PFH fragment by torsion tests as linear, and determine its rigidity:

$$C_i = \frac{M_i^{\max}}{\Delta\phi_i^{\max}}, \tag{1}$$

where C_i is the rigidity for the i -th cycle; M_i^{\max} is the maximum loading for the i -th cycle; $\Delta\phi_i^{\max}$ is the maximum magnitude of deformation of the i -th cycle.

Taking into consideration statistically treated experimental data (Tables 1–3), the elasticity module at the shear of the material of a pressure fire hose by torsion tests is shown in Table 4.

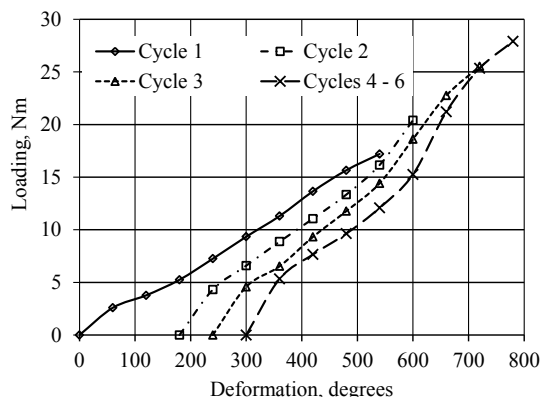


Fig. 2. Diagrams of loading the experimental fragments of a fire hose at torsion (pressure in a hose $P_1=0.2$ MPa)

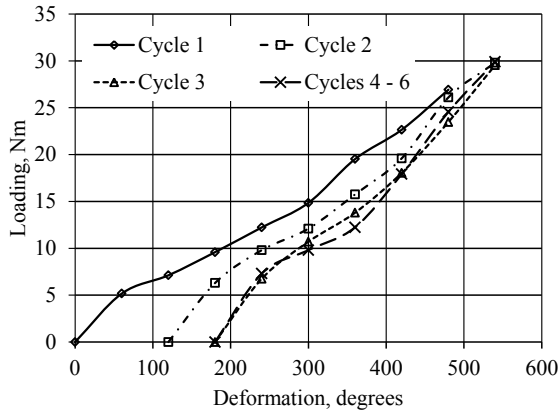


Fig. 3. Diagrams of loading of experimental fragments of a fire hose (pressure in a hose $P_2=0.4$ MPa)

Diagrams in Fig. 4 correspond to the statistically treated results of torsion tests of a pressure fire hose at internal pressure $P_3=0.6$ MPa.

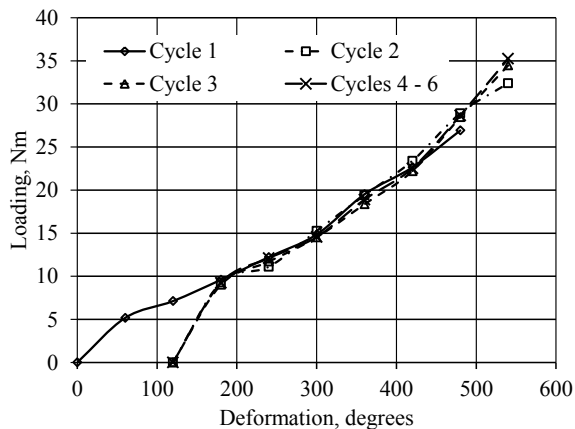


Fig. 4. Diagrams of loading the experimental fragments of a fire hose at torsion (pressure in a hose $P_3=0.6$ MPa)

Table 4

The rigidity of material of the PFH fragment with internal diameter $d=77$ mm at shear deformation

Cycle	The rigidity of fragment C_i , Nm/degree		
	Pressure $P_1=0.2$ MPa	Pressure $P_2=0.4$ MPa	Pressure $P_3=0.6$ MPa
Cycle 1	0.0319	0.0561	0.0624
Cycle 2	0.0486	0.0710	0.0771
Cycle 3	0.0532	0.0820	0.0821
Cycles 4–6	0.0581	0.0831	0.0839

Thus, the elasticity modules first increase and are stabilized during tests 4–6.

4. 3. Experimental studies of elastic properties at the shear of the material of a pressure fire hose in torsion tests

Experiments on determining dissipative properties at the shear of the material of a pressure fire hose by torsion tests were carried out simultaneously with determining elastic characteristics.

The results of studying the statistical treatment of the material of a pressure fire hose by torsion tests at internal pressure $P_1=0.2$ MPa are shown in Table 5, $P_2=0.4$ MPa – in Table 6, and $P_3=0.6$ MPa – in Table 7

The initial (1) loading cycle (Fig. 5) was carried out with a non-deformed fragment of a fire hose. The maximum magnitude of deformation was $\Delta\phi_1^{\max}=540^\circ$ at loading $M_1^{\max}=17.2$ Nm. After unloading, residual deformation of the fragment was $\Delta\phi_1^{\text{res}}=180^\circ$.

Table 5

Results of experimental tests of PFH ($P_1=0.2$ MPa)

Angle of torsion ϕ , degrees	Pressure in a hose, $P_1=0.2$ MPa							
	Torque M , Nm							
	Cycle 1		Cycle 2		Cycle 3		Cycle 4–6	
	L	U	L	U	L	U	L	U
0	0	–	–	–	–	–	–	–
60	2.59	–	–	–	–	–	–	–
120	3.77	–	–	–	–	–	–	–
180	5.25	0	0	–	–	–	–	–
240	7.25	0.55	4.31	0	0	–	–	–
300	9.34	1.42	6.59	1.47	4.58	0	0	0
360	11.3	2.48	8.87	2.86	6.53	1.22	5.33	1.26
420	13.65	4.32	11.05	5.94	9.32	3.54	7.65	3.16
480	15.65	9.24	13.34	7.68	11.77	6.34	9.63	6.12
540	17.2	17.2	16.15	11.36	14.41	9.72	12.08	9.24
600	–	–	20.4	20.4	18.61	14.38	15.25	12.28
660	–	–	–	–	22.75	18.22	21.2	15.12
720	–	–	–	–	25.52	25.52	25.34	20.36
780	–	–	–	–	–	–	27.9	27.9

During the repeated cycle (Fig. 6), which was conducted 2 minutes after cycle 1, the maximum magnitude of deformation was $\Delta\phi_2^{\max}=420^\circ$ at loading $M_2^{\max}=20.4$ Nm. After unloading, residual deformation of the fragment was $\Delta\phi_2^{\text{res}}=60^\circ$.

At loading 3 (Fig. 7), the maximum magnitude of deformation was $\Delta\phi_3^{\max}=480^\circ$ at loading $M_3^{\max}=25.52$ Nm. After unloading, residual deformation of the fragment was $\Delta\phi_3^{\text{res}}=60^\circ$.

Numerical parameters of the following two loading cycles (4) to (6) (Fig. 8), that were carried out at similar two-minute intervals, almost do not differ from each other, which enabled us to average their values. The maximum magnitude of deformation was $\Delta\phi_{4-6}^{\max}=480^\circ$ at loading $M_{4-6}^{\max}=27.9$ Nm. There was no residual deformation after unloading.

Results of torsion tests of the material of a pressure fire at internal pressure $P_2=0.4$ MPa are given in Table 6.

The initial (1) loading cycle (Fig. 9) was carried out with a non-deformed fragment of a fire hose. The maximum magnitude of deformation was $\Delta\phi_1^{\max}=480^\circ$ at loading $M_1^{\max}=26.92$ Nm. Residual deformation after unloading was $\Delta\phi_1^{\text{res}}=120^\circ$.

At repeated loading (Fig. 10), which was carried out 2 minutes after the first one, the maximum magnitude of deformation was $\Delta\phi_2^{\max}=420^\circ$ at loading $M_2^{\max}=29.8$ Nm. Residual deformation after loading was $\Delta\phi_2^{\text{res}}=60^\circ$.

At loading 3 (Fig. 11), the maximum magnitude of deformation was $\Delta\phi_3^{\max}=360^\circ$ at loading $M_3^{\max}=29.8$ Nm. There was no residual deformation after unloading.

Numerical parameters of the following two loading cycles (4)–(6) (Fig. 12) that were carried out at similar two-minute intervals almost do not differ from each other, which enables us to average their values. The maximum magnitude of deformation was $\Delta\phi_{4-6}^{\max}=360^\circ$ at loading $M_{4-6}^{\max}=29.9$ Nm. There was no residual deformation after unloading.

Table 6

Results of experimental tests of the PFH ($P_2=0.4$ MPa)

Torsion angle φ , degree	Pressure in a hose, $P_2=0.4$ MPa							
	Torque M , Nm							
	Cycle 1		Cycle 2		Cycle 3		Cycles 4-6	
	L	U	L	U	L	U	L	U
0	0	-	-	-	-	-	-	-
60	5.17	-	-	-	-	-	-	-
120	7.12	0	0	-	-	-	-	-
180	9.59	0.69	6.3	0	0	0	0	0
240	12.23	2.48	9.8	0.71	6.75	0.67	7.3	0.56
300	14.85	7.34	12.1	1.96	10.7	2.18	9.81	2.48
360	19.52	12.28	15.75	6.32	13.8	4.82	12.24	5.36
420	22.65	18.21	19.6	11.04	18.05	10.04	17.93	10.21
480	26.92	26.92	26.1	19.23	23.47	18.38	24.55	16.77
540	-	-	29.8	29.8	29.53	29.53	29.9	29.9

Results of torsion tests of the material of a pressure fire hose at internal pressure $P_3=0.6$ MPa are given in Table 7.

The initial (1) loading cycle (Fig. 13) was carried out with a non-deformed fragment of a fire hose. The maximum magnitude of deformation was $\Delta\phi_1^{\max} = 480^\circ$ at loading $M_1^{\max} = 29.95$ Nm. Residual information after unloading was $\Delta\phi_1^{\text{res}} = 120^\circ$.

Table 7

Results of experimental tests of the PFH ($P_3=0.6$ MPa)

Torsion angle φ , degrees	Pressure in a hose, $P_3=0.6$ MPa							
	Torque M , Nm							
	Cycle 1		Cycle 2		Cycle 3		Cycles 4-6	
	L	U	L	U	L	U	L	U
0	0	-	-	-	-	-	-	-
60	6.4	-	-	-	-	-	-	-
120	8.64	0	0	0	0	0	0	0
180	11.2	0.72	9.29	1.69	9.01	1.29	9.24	1.92
240	14	2.37	11.1	3.57	11.7	3.48	12.1	4.56
300	16.72	6.35	15.27	7.38	14.52	9.36	14.56	8.94
360	20.37	11.48	19.41	11.78	18.37	14.32	18.9	14.78
420	23.71	18.49	23.4	17.87	22.2	19.81	22.53	19.86
480	29.95	29.95	28.91	22.39	28.46	24.68	28.67	26.24
540	-	-	32.4	32.4	34.47	34.47	35.24	35.24

At repeated loading (Fig. 14), which was carried out 2 minutes after the first one, the maximum magnitude of deformation was $\Delta\phi_2^{\max} = 420^\circ$ at loading $M_2^{\max} = 32.4$ Nm. There was no residual deformation after unloading.

At loading 3 (Fig. 15), the maximum magnitude of deformation was $\Delta\phi_3^{\max} = 420^\circ$ at loading $M_3^{\max} = 34.47$ Nm. There was no residual deformation after unloading.

Numerical parameters of the following two loading cycles (4) to (6) (Fig. 16) that were carried out at similar two-minute intervals almost do not differ from each other, which enabled us to average their values. The maximum magnitude of deformation was $\Delta\phi_{4-6}^{\max} = 420^\circ$ at loading $M_{4-6}^{\max} = 35.24$ Nm. There was no residual deformation after unloading.

4. 2. Results of experimental studies of elastic properties at the shear of the material of a pressure fire hose in torsion tests

The results of statistically treated experimental studies of the PFH material by torsion tests at internal pressure $P_1=0.2$ MPa in Table 5, $P_2=0.4$ MPa in Table 6, and $P_3=0.6$ MPa in Table 7 were approximated by the corresponding trends, the diagrams of which are shown in Fig. 5-16.

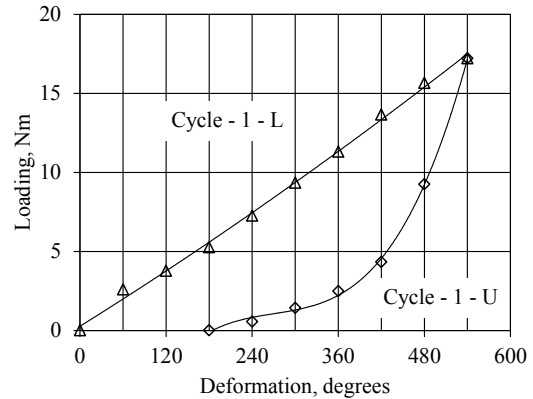


Fig. 5. Diagrams of the trends of cycle 1: L – loading; U – unloading (pressure in a hose $P_1=0.2$ MPa)

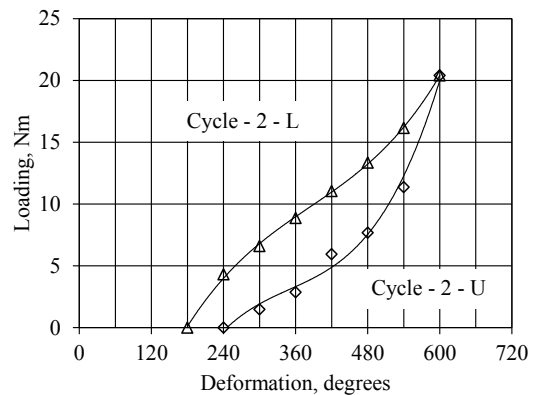


Fig. 6. Diagrams of the trends of cycle 2: L – loading; U – unloading (pressure in a hose $P_1=0.2$ MPa)

Diagrams in Fig. 7 correspond to the polynomial trends of cycle 3 of loading-unloading of the fragments of PFH materials.

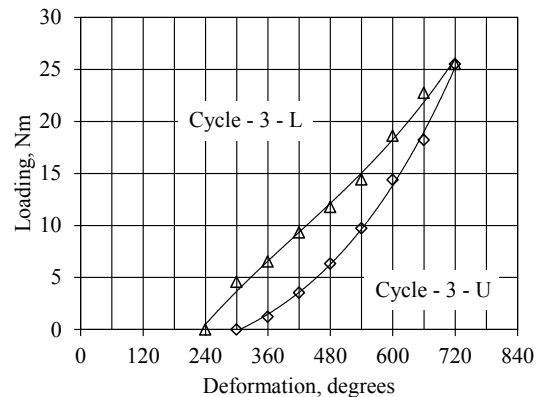


Fig. 7. Diagrams of the trends of cycle 3: L – loading; U – unloading (pressure in a hose $P_1=0.2$ MPa)

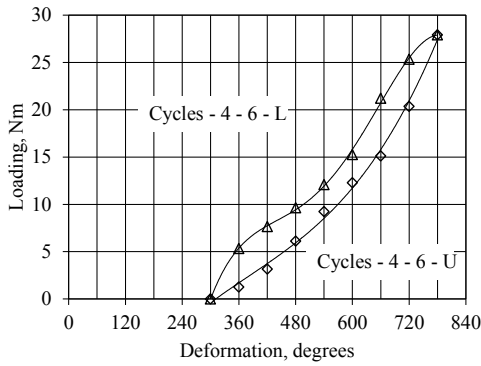


Fig. 8. Diagrams of the trends of cycle 4–6:
L – loading; U – unloading (pressure in a hose $P_1=0.2$ MPa)

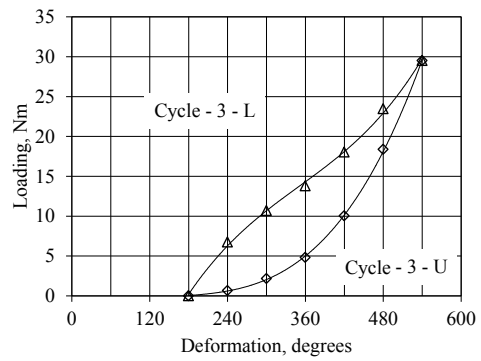


Fig. 11. Diagrams of the trends of cycle 3:
L – loading; U – unloading (pressure in a hose $P_2=0.4$ MPa)

The results of testing at internal pressure $P_2=0.4$ MPa were approximated using a similar procedure, Fig. 9–12.

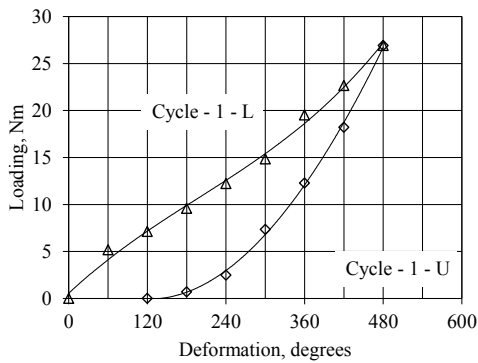


Fig. 9. Diagrams of the trends of cycle 1:
L – loading; U – unloading (pressure in a hose $P_2=0.4$ MPa)

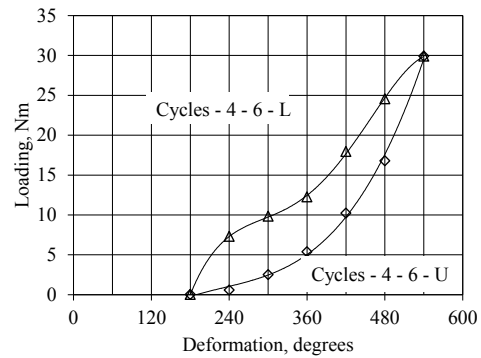


Fig. 12. Diagrams of the trends of cycles 4–6:
L – loading; U – unloading (pressure in a hose $P_2=0.4$ MPa)

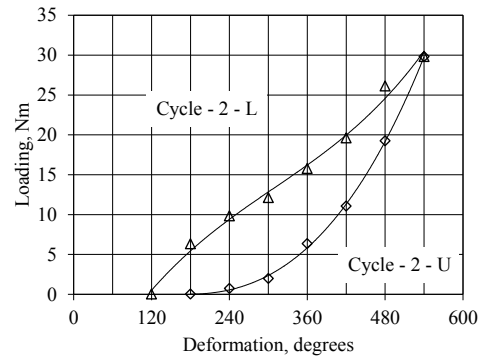


Fig. 10. Diagrams of trends of cycle 2:
L – loading; U – unloading (pressure in a hose $P_2=0.4$ MPa)

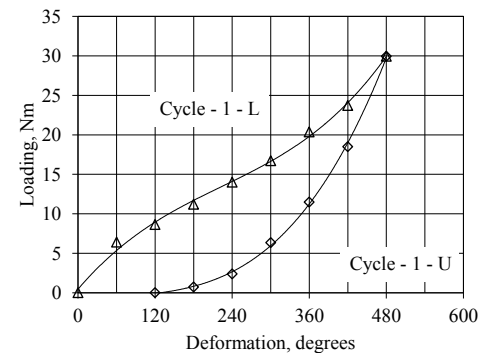


Fig. 13. Diagrams of the trends of cycle 1:
L – loading; U – unloading (pressure in a hose $P_3=0.6$ MPa)

Diagrams in Fig. 11 correspond to the polynomial trends of cycle 3 of loading-unloading of the fragments of PFH materials.

The results of testing at internal pressure $P_3=0.6$ MPa were approximated using a similar procedure, Fig. 13–16.

Diagrams in Fig. 15 correspond to the polynomial trends of cycle 3 of loading-unloading of the fragments of PFH material.

The dependences obtained by using the Microsoft Excel 2007 tabular processor were approximated by a polynomial trend line. Types of trend lines were chosen based on the calculated value of the determining factor, which characterizes the degree of proximity of the specified lines to the source data.

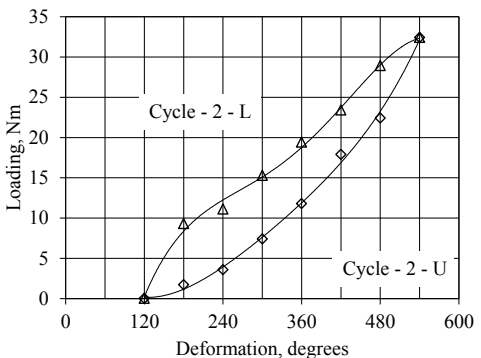


Fig. 14. Diagrams of the trends of cycle 2:
L – loading; U – unloading (pressure in a hose $P_3=0.6$ MPa)

Among the possible types of trend lines, an exponential, a linear, a logarithmic, and power lines were explored.

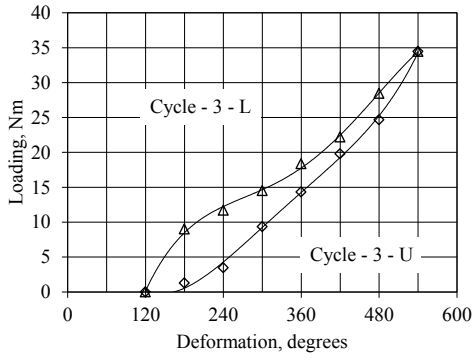


Fig. 15. Diagrams of the trends of cycle 3:
L – loading; U – unloading
(pressure in a hose $P_3=0.6$ MPa)

Accordingly, the highest value, which approached unity, was obtained for the power trend line.

The resulting trend lines describe the corresponding equations that are shown in Table 8.

Energy (A_d), which is accumulated in the sample and corresponds to dissipative properties of the material of the fire hose fragment, is determined by the area of the hysteresis loop as the difference of works spent during loading (A_l) and subsequent unloading (A_u) of the sample

$$A_d = A_l - A_u = \int_{\phi_{li}}^{\phi_{lf}} M_l(\phi) d(\phi) - \int_{\phi_{ui}}^{\phi_{uf}} M_u(\phi) d(\phi), \quad (2)$$

where $M_l(\phi)$ is the equation of dependence of operating moment on deformation (torsion angle) of the hose fragment at its loading; $M_u(\phi)$ is the equation of dependence of operating moment on deformation (torsion angle) at its unloading; ϕ_{li}, ϕ_{lf} is the lower (upper) boundaries of integration, which correspond to the initial point of loading; ϕ_{ui}, ϕ_{uf} is the lower (upper) boundaries of integration which corresponds to the final unloading point.

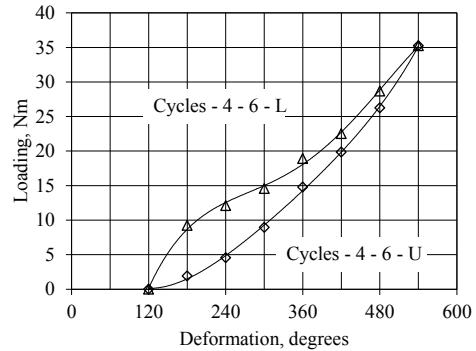


Fig. 16. Diagrams of the trends of cycles 4–6:
L – loading; U – unloading (pressure in a hose $P_3=0.6$ MPa)

Table 8

Regression equations and degree of processes reliability

Cycle No.	Equations of the dependence of operating moment (Y) on deformation (torsion angle) (X)	Reliability degree
$P_1=0.2$ MPa		
1-L	$Y = 7E - 6 \cdot X^2 + 0.0284 \cdot X + 0.2697$	$R^2 = 0.9972$
1-U	$Y = 7E - 7 \cdot X^3 - 0.0006 \cdot X^2 + 0.165 \cdot X - 15.065$	$R^2 = 0.999$
2-L	$Y = 3E - 7 \cdot X^3 - 0.0004 \cdot X^2 + 0.187 \cdot X - 22.573$	$R^2 = 0.9994$
2-U	$Y = 7E - 7 \cdot X^3 - 0.0008 \cdot X^2 + 0.2904 \cdot X - 35.842$	$R^2 = 0.9912$
3-L	$Y = 3E - 7 \cdot X^3 - 0.0004 \cdot X^2 + 0.187 \cdot X - 22.573$	$R^2 = 0.9952$
3-U	$Y = 9E - 8 \cdot X^3 - 3E - 5 \cdot X^2 + 0.018 \cdot X - 5.2156$	$R^2 = 0.9981$
4-6-L	$Y = -3E - 9 \cdot X^4 + 6E - 6 \cdot X^3 - 0.005 \cdot X^2 + 1.749 \cdot X - 219.68$	$R^2 = 0.9991$
4-6-U	$Y = 2E - 7 \cdot X^3 - 0.0002 \cdot X^2 + 0.1107 \cdot X - 20.122$	$R^2 = 0.9963$
$P_2=0.4$ MPa		
1-L	$Y = 2E - 7 \cdot X^3 - 0.0001 \cdot X^2 + 0.0653 \cdot X + 0.5484$	$R^2 = 0.9954$
1-U	$Y = -5E - 8 \cdot X^3 - 0.0002 \cdot X^2 - 0.0588 \cdot X - 3.5143$	$R^2 = 0.9985$
2-L	$Y = 4E - 7 \cdot X^3 - 0.0003 \cdot X^2 + 0.1559 \cdot X - 14.121$	$R^2 = 0.9931$
2-U	$Y = 3E - 7 \cdot X^3 - 3E - 0.5 \cdot X^2 - 0.0182 \cdot X + 2.4667$	$R^2 = 0.9993$
3-L	$Y = 7E - 7 \cdot X^3 - 0.0007 \cdot X^2 + 0.3176 \cdot X - 37.138$	$R^2 = 0.9986$
3-U	$Y = 5E - 7 \cdot X^3 - 0.002 \cdot X^2 + 0.0453 \cdot X - 3.0864$	$R^2 = 0.9998$
4-6-L	$Y = -9E - 9 \cdot X^4 + 1E - 5 \cdot X^3 - 0.0075 \cdot X^2 + 1.77 \cdot X - 145.94$	$R^2 = 0.9998$
4-6-U	$Y = 8E - 7 \cdot X^3 - 0.0005 \cdot X^2 + 0.1417 \cdot X - 13.024$	$R^2 = 0.9998$
$P_3=0.6$ MPa		
1-L	$Y = 4E - 7 \cdot X^3 - 0.0003 \cdot X^2 + 0.0954 \cdot X + 0.4496$	$R^2 = 0.9969$
1-U	$Y = 4E - 7 \cdot X^3 - 8E - 5 \cdot X^2 + 0.0124 \cdot X - 1.0843$	$R^2 = 0.9992$
2-L	$Y = -4E - 9 \cdot X^4 + 6E - 6 \cdot X^3 - 0.0031 \cdot X^2 + 0.6959 \cdot X - 48.744$	$R^2 = 0.9966$
2-U	$Y = 2E - 9 \cdot X^4 - 2E - 6 \cdot X^3 + 0.001 \cdot X^2 - 0.1711 \cdot X + 9.3312$	$R^2 = 0.9975$
3-L	$Y = -4E - 9 \cdot X^4 + 6E - 6 \cdot X^3 - 0.0029 \cdot X^2 + 0.6895 \cdot X - 49.143$	$R^2 = 0.9988$
3-U	$Y = 3E - 9 \cdot X^4 - 5E - 6 \cdot X^3 - 0.0023 \cdot X^2 - 0.4098 \cdot X + 23.91$	$R^2 = 0.9982$
4-6-L	$Y = -4E - 9 \cdot X^4 + 5E - 6 \cdot X^3 - 0.0029 \cdot X^2 + 0.6836 \cdot X - 49.041$	$R^2 = 0.9983$
4-6-U	$Y = 2E - 9 \cdot X^4 - 2E - 6 \cdot X^3 + 0.0011 \cdot X^2 - 0.1781 \cdot X + 9.437$	$R^2 = 0.9993$

For further calculations, it is advisable to determine the dissipative properties of a fire hose by the dimensionless ratio, or dissipation factor:

$$\beta = \frac{A_d}{A_u} \tag{3}$$

The equations of corresponding trends were obtained after statistical treatment of the results of the study by Microsoft Excel 2007 and respectively determined by loading energy (A_l) and of the i -th cycle, unloading energy (A_u) of the i -th cycle, and dissipation factor (β) of the i -th cycle.

Table 9

Summary table of the results of calculations of some mechanical properties of a fire hose at shear

Characteristic	Designation	Cycle			
		Cycle 1	Cycle 2	Cycle 3	Cycles 4-6
Pressure in a hose $P_1=0.2$ MPa					
Maximum moment	M_i^{max} , Nm	17.20	20.4	25.52	27.90
Maximum deformation	$\Delta\phi_i^{max}$, degree	540	420	480	480
Residual deformation	$\Delta\phi_i^{res}$, degree	180	60	60	0
Elasticity module	G_i , MPa	1.67	2.54	2.78	3.04
Dissipation factor	β_i	0.648	0.373	0.353	0.225
Pressure in a hose $P_2=0.4$ MPa					
Maximum moment	M_i^{max} , Nm	26.92	29.80	29.53	29.90
Maximum deformation	$\Delta\phi_i^{max}$, degree	480	420	360	360
Residual deformation	$\Delta\phi_i^{res}$, degree	120	60	0	0
Elasticity module	G_i , MPa	2.93	3.71	4.29	4.35
Dissipation factor	β_i	0.477	0.472	0.450	0.225
Pressure in a hose $P_3=0.6$ MPa					
Maximum moment	M_i^{max} , Nm	29.95	32.40	34.47	35.24
Maximum deformation	$\Delta\phi_i^{max}$, degree	480	420	420	420
Residual deformation	$\Delta\phi_i^{res}$, degree	120	0	0	0
Elasticity module	G_i , MPa	3.26	4.03	4.29	4.39
Dissipation factor	β_i	0.538	0.283	0.258	0.207

The generalization of the conducted set of experimental tests is given in Table 9, which consolidates the averaged estimates of strength and elasticity at the shear of the material of a pressure fire hose of "T" type with the inner diameter of 77 mm in torsion tests.

5. Discussion of the results of studying the elastic and dissipative properties of pressure fire hoses

A series of experimental determining elastic and dissipative properties at the shear of the PFH material of the "T"

type with the internal diameter of 77 mm by torsion tests established that significant initial hysteresis of a fragment of a fire hose at torsion with different internal pressure (P) in cycle 1 (Fig. 5, 9, 13), cycle 2 (Fig. 6, 10, 14), in cycles 3 (Fig. 7, 11, 15), cycle 4-6 (Fig. 8, 12, 16) significantly decreases. This, together with a decrease in residual deformations and stabilization of elastic properties (Table 9) approximates to elastic the behavior of material of a hose material at torsion.

Without resorting to consideration of the physical and mechanical properties of the PFH material and its structural features (this issue will be considered in further research), the presented figures reflect the overall picture of experimental data regarding a "T" type hose with the internal diameter of 77 mm.

These tests are aimed only at a simplified assessment of the PFH reliability. Their task does not include determining the physical and mechanical properties of the PFH material. This limits the possibility of conducting theoretical research using the finite element method.

The conducted tests were limited to the research of only one hose type, in this case, the extent of its wear was not taken into consideration.

These restrictions can be eliminated by research into different types of hoses with an arbitrary term of operation and statistical treatment of the results.

Reliable and safe use of the PFH, which is determined by hydraulic tests for tightness during scheduled inspections determines only the integrity and tightness of pressure fire hoses.

Further development of relevant studies is an experimental analysis of the effects of cyclic deformation, as well as the impact of high temperatures on the physical and mechanical properties of the PFH material.

These studies require the development of both a new procedure of conducting experiments and the manufacturing of appropriate equipment.

6. Conclusions

1. Experimental studies on determining the elastic properties at the shear of the PFH material by torsion tests revealed that the elasticity module of the material of a hose is stabilized at the level of 3.04 MPa for P_1 , 4.35 MPa for P_2 , 4.39 MPa for P_3 . At the same time, the magnitude of the elasticity module at almost the same loading range (17 ± 35 Nm, taking into consideration pressure (P)), is quite dependent on the loading "history", that is, in the first two, three test modes, the corresponding rigidity and elasticity modulus increased and only then stabilized at a significant decrease in residual deformations ($5\div 0$ mm) in the following modes.

2. Experimental studies on determining the dissipative properties of the PFH by torsion tests established that the coefficient of dissipation of the material of a hose stabilized at the level of $0.225\div 0.225$. In this case, its magnitude at almost the same loading range ($17\div 35$ Nm, taking into account pressure (P)), was decreasing steadily and stabilized only in the following modes.

References

1. Kovalenko, R., Kalynovskiy, A., Nazarenko, S., Kryvoshei, B., Grinchenko, E., Demydov, Z. et. al. (2019). Development of a method of completing emergency rescue units with emergency vehicles. Eastern-European Journal of Enterprise Technologies, 4 (3 (100)), 54-62. doi: <https://doi.org/10.15587/1729-4061.2019.175110>

2. Dubinin, D., Korytchenko, K., Lisnyak, A., Hrytsyna, I., Trigub, V. (2017). Numerical simulation of the creation of a fire fighting barrier using an explosion of a combustible charge. *Eastern-European Journal of Enterprise Technologies*, 6 (10 (90)), 11–16. doi: <https://doi.org/10.15587/1729-4061.2017.114504>
3. Tiutiunyk, V. V., Ivanets, H. V., Tolkunov, I. A., Stetsyuk, E. I. (2018). System approach for readiness assessment units of civil defense to actions at emergency situations. *Scientific Bulletin of National Mining University*, 1, 99–105. doi: <https://doi.org/10.29202/nvngu/2018-1/7>
4. Larin, O., Chernobay, G., Kohanenko, V., Nazarenko, S. (2015). A study of longitudinal stiffness of t-type fire hoses with 77mm diameter with structural elements fire hose. *Visnyk Natsionalnoho tekhnichnoho universytetu «Kharkivskiy politekhnichnyi instytut»*. Seriya: Novi rishennia v suchasnykh tekhnolohiyakh, 39, 41–46.
5. Fedorko, G., Molnar, V., Dovica, M., Toth, T., Fabianova, J. (2015). Failure analysis of irreversible changes in the construction of the damaged rubber hoses. *Engineering Failure Analysis*, 58, 31–43. doi: <https://doi.org/10.1016/j.engfailanal.2015.08.042>
6. Cho, J.-R., Yoon, Y.-H. (2016). Large deformation analysis of anisotropic rubber hose along cyclic path by homogenization and path interpolation methods. *Journal of Mechanical Science and Technology*, 30 (2), 789–795. doi: <https://doi.org/10.1007/s12206-016-0134-5>
7. Cho, J. R., Yoon, Y. H., Seo, C. W., Kim, Y. G. (2015). Fatigue life assessment of fabric braided composite rubber hose in complicated large deformation cyclic motion. *Finite Elements in Analysis and Design*, 100, 65–76. doi: <https://doi.org/10.1016/j.finel.2015.03.002>
8. Traxl, R., Mungenast, D., Schennach, O., Lackner, R. (2019). Mechanical performance of textile-reinforced hoses assessed by a truss-based unit cell model. *International Journal of Engineering Science*, 141, 47–66. doi: <https://doi.org/10.1016/j.ijengsci.2019.05.006>
9. Motorin, L. V., Stepanov, O. S., Bratolyubova, E. V. (2011). The simplified mathematical model for strength calculation of pressure fire hoses under hydraulic influence. *Tehnologiya tekstil'noy promyshlennosti*, 1, 126–133.
10. Kobeyeva, N. M., Togatayev, T. U., Yeldiyar, G. K., Kuralbayeva, A. N., Zholayeva, N. Kh., Sadyrbayeva, I. R. (2016). Geometrical densities according to warp and weft yarns of fabric reinforcing framework of fire hoses. *Science and world*, 1 (5 (33)), 90–91.
11. Larin, O. O. (2015). Probabilistic Model of Fatigue Damage Accumulation in Rubberlike Materials. *Strength of Materials*, 47 (6), 849–858. doi: <https://doi.org/10.1007/s11223-015-9722-3>
12. Larin, A. A., Vyazovichenko, Y. A., Barkanov, E., Itskov, M. (2018). Experimental Investigation of Viscoelastic Characteristics of Rubber-Cord Composites Considering the Process of Their Self-Heating. *Strength of Materials*, 50 (6), 841–851. doi: <https://doi.org/10.1007/s11223-019-00030-7>
13. Larin, O., Morozov, O., Nazarenko, S., Chernobay, G., Kalynovskiy, A., Kovalenko, R. et. al. (2019). Determining mechanical properties of a pressure fire hose the type of «T». *Eastern-European Journal of Enterprise Technologies*, 6 (7 (102)), 63–70. doi: <https://doi.org/10.15587/1729-4061.2019.184645>
14. Haseeb, A. S. M. A., Jun, T. S., Fazal, M. A., Masjuki, H. H. (2011). Degradation of physical properties of different elastomers upon exposure to palm biodiesel. *Energy*, 36 (3), 1814–1819. doi: <https://doi.org/10.1016/j.energy.2010.12.023>
15. Lee, G.-C., Kim, H.-E., Park, J.-W., Jin, H.-L., Lee, Y.-S., Kim, J.-H. (2011). An experimental study and finite element analysis for finding leakage path in high pressure hose assembly. *International Journal of Precision Engineering and Manufacturing*, 12 (3), 537–542. doi: <https://doi.org/10.1007/s12541-011-0067-y>
16. Pavloušková, Z., Klakurková, L., Man, O., Čelko, L., Švejcar, J. (2015). Assessment of the cause of cracking of hydraulic hose clamps. *Engineering Failure Analysis*, 56, 14–19. doi: <https://doi.org/10.1016/j.engfailanal.2015.05.014>